JACS
JOURNAL OF THE AMERICAN CHEMICAL SOCIETY
Cite This: J. Am. Chem. Soc. 2018, 140, 12756−12759
Communication
pubs.acs.org/JACS

Stable Mixed-Valent Complexes Formed by Electron Delocalization Across Hydrogen Bonds of Pyrimidinone-Linked Metal Clusters

Tyler M. Porter,[†] Gavin P. Heim,[†] and Clifford P. Kubiak*

Department of Chemistry and Biochemistry, University of California, San Diego, 9500 Gilman Drive, La Jolla, California 92093-0358, United States

Supporting Information

ABSTRACT: Electron transfer across a mixed-valent hydrogen-bonded self-dimer of oxo-centered triruthenium clusters bridged by a pair of 4(3*H*)-pyrimidinones is reported. Spectroelectrochemical studies in methylene chloride reveal that **1** rapidly self-dimerizes upon one-electron reduction, forming the strongly coupled mixed-valent hydrogen-bonded dimer $(\mathbf{1}_2)^-$. In the mixed-valent state, significantly broadened, partially coalesced ν(CO) bands are observed, allowing estimation of the electron transfer rate (k_{ET}) by an optical Bloch line shape analysis. Simulation of the FTIR line shapes provides an estimate of k_{ET} on the order of 10^{11} s^{-1}, indicating a highly delocalized electronic structure *across* the hydrogen bonds. These findings are supported by the determination of the formation constant (K_{MV}) for $(\mathbf{1}_2)^-$, which is found to be on the order of 10^6 M^{-1}, or nearly 4 orders of magnitude higher than that for the neutral isovalent dimer ($\mathbf{1}_2$). This represents a stabilization of approximately 5.7 kcal/mol (1980 cm^{-1}) arising from electron exchange across the hydrogen bonds in the mixed-valent state. Significantly, an enormous intensity enhancement of the amide ν(NH) band (3300 cm^{-1}) of $(\mathbf{1}_2)^-$ is observed, supporting strong mixing of the bridging ligand vibrational modes with the electronic wave function of the mixed-valent state. These findings demonstrate strong donor−bridge−acceptor coupling and that highly delocalized electronic structures can be attained in hydrogen-bonded systems, which are often considered to be too weakly bound to support strong electronic communication.

Electron transfer (ET) lies at the core of chemical and biological processes.[1−7] In biological systems, ET often follows pathways that favor donor−acceptor overlap between intervening redox-active amino acid side chains over tunneling.[3−13] These interactions allow for distances of ET upward of 30 Å to be traversed in nanoseconds.[3,9] To better understand what effects govern long-range ET in supramolecular systems, it is crucial to understand what mechanisms drive donor−acceptor overlap when redox sites are bridged by non-covalent interactions.

We recently reported a methodology to compare the strengths of hydrogen bonds in mixed-valent hydrogen-bonded complexes both in the presence and in the absence of electron exchange.[14] By employing hydrogen bonds of isonicotinic acid (Figure S3) to link two Ru_3O redox centers, we found that the stabilities of the mixed-valent states were significantly greater than those of the two isovalent states.[14] Determination of the formation constants for the hydrogen bonds in all of the redox states showed that electron exchange imparts about 3−5 kcal mol^{-1} of stability to the hydrogen bond relative to the isovalent states. Applying a similar methodology herein, we report on the observation of a mixed-valent hydrogen-bonded dimer of oxo-centered triruthenium clusters bridged by hydrogen bonds of the pyrimidine 4(3*H*)-pyrimidinone (Figure 1).

Complex **1** was synthesized by treatment of $Ru_3O(OAc)_6(CO)(py)(MeOH)$ with a stoichiometric amount of 4(3*H*)-pyrimidinone in a dichloromethane DCM/MeOH solution. Investigation of the mechanism of ground-state ET proceeded by measurement of the cyclic voltammogram (CV).

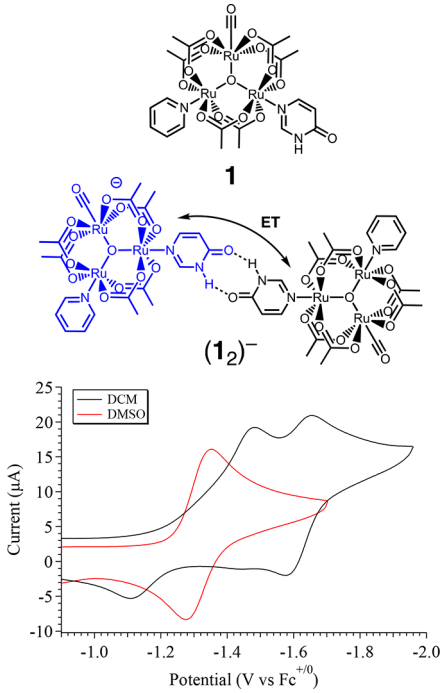

Figure 1. (top) Structures of the free monomer **1** and the hydrogen-bonded dimer $(\mathbf{1}_2)^-$. (bottom) Cyclic voltammograms of **1** (2.00 mM) at 100 mV/s in DCM (black) and DMSO (red) at 23 °C. Potentials are referenced to the $Fc^{+/0}$ redox couple using an internal standard of ferrocene.

Received: August 28, 2018
Published: September 28, 2018

DOI: 10.1021/jacs.8b09273
J. Am. Chem. Soc. 2018, 140, 12756−12759

By the use of a single-compartment electrochemical cell consisting of a glassy carbon working electrode, a platinum counter electrode, and a Ag/AgCl reference electrode, the CV of **1** was recorded in a solution of DCM containing 0.1 M tetrabutylammonium hexafluorophosphate ($TBAPF_6$) as the supporting electrolyte (Figure 1). Upon scanning to reducing potentials, one quasi-reversible response and one reversible response are observed at −1.45 and −1.65 V vs $Fc^{+/0}$ respectively. On the return sweep, two oxidative responses are observed, one corresponding to the reoxidation of the species reduced at −1.65 V vs $Fc^{+/0}$, which is followed by an irreversible response at −1.08 V vs $Fc^{+/0}$. Differential pulse voltammetry confirmed that all of the redox features are single-electron processes (Figure S2). The electrochemical behavior was additionally observed to be both solvent- and scan-rate-dependent. As the scan rate is increased, the second reduction and irreversible oxidation are both observed to nearly vanish while the first reduction ($E_{1/2}$ = −1.45 V vs $Fc^{+/0}$) gains considerable reversibility (Figure S2). Upon dissolution of **1** in dimethyl sulfoxide (DMSO), a solvent known to disrupt hydrogen bonds, only a single reversible response is observed at $E_{1/2}$ = −1.32 V vs $Fc^{+/0}$ (red CV in Figure 1). These results suggest that a stable mixed-valent dimer is formed in DCM but not in DMSO.[14−16] The electrochemistry is best described as following an ECE mechanism, in which after a one-electron reduction (E) a chemical step (C) occurs (self-dimerization), which is then followed by a second reduction (E). In the CV of complex **1**, the first quasi-reversible wave ($E_{1/2}$ = −1.45 V vs $Fc^{+/0}$) corresponds to reduction of neutral monomers to form anionic monomers, $(\mathbf{1})^-$. These then rapidly dimerize with neutral monomers (**1**) in the diffusion layer, forming mixed-valent hydrogen-bonded dimers, $(\mathbf{1}_2)^-$. At the second, reversible wave ($E_{1/2}$ = −1.65 V vs $Fc^{+/0}$), the mixed-valent hydrogen-bonded dimers are reduced by a second electron to their isovalent, dianionic hydrogen-bonded state, $(\mathbf{1}_2)^{2-}$. Upon reversal of the scan direction, the first oxidative feature near −1.65 V vs $Fc^{+/0}$ corresponds to oxidation of the isovalent, doubly reduced dimers $(\mathbf{1}_2)^{2-}$ to the mixed-valent hydrogen-bonded dimers $(\mathbf{1}_2)^-$. Because of electron exchange across the hydrogen bonds, this state is sufficiently stable to persist until its subsequent oxidation at −1.08 V vs $Fc^{+/0}$, whereby neutral dimers, $\mathbf{1}_2$, are formed and then rapidly dissociate into two neutral monmers, **1**.

The stability of the mixed-valent state is expressed by the comproportionation constant (eq 1):

$$K_C = e^{nF\Delta E/RT} \quad (1)$$

Here one needs to know only the difference between the potentials relating the two isovalent states to the mixed-valence state. In complex **1**, this is taken as the difference between the two oxidative features on the return sweep, where splittings of 460 ±10 mV correspond to a comproportionation constant of 7.0×10^7. These splittings are 75 mV larger than those observed in the isonicotinic acid systems described earlier (ΔE = 385 mV, $K_C = 3.2 \times 10^6$; Figure S3)[14,16] and indicate the formation of a highly stable mixed-valent anion with respect to the two isovalent states.

These observations are further supported by determination of the formation constants for the relevant redox states. In general, any mixed-valent hydrogen-bonded system can be described by a series of four dimerization equilibria (Figure 2). K_D and K_{2-} are the equilibrium constants for the two isovalent species, which describe the self-dimerization of the neutral and

$$\begin{aligned} M + M &\rightleftharpoons M_2 & K_D \\ M + (M)^- &\rightleftharpoons (M_2)^- & K_{MV} \\ (M)^- + (M)^- &\rightleftharpoons (M_2)^{2-} & K_{2-} \\ M_2 + (M_2)^{2-} &\rightleftharpoons 2\,(M_2)^- & K_C \end{aligned}$$

Figure 2. Dimerization equilibria of a mixed-valent hydrogen-bonded system in solution.

one-electron-reduced clusters, respectively. K_C is the comproportionation constant, and K_{MV} is the equilibrium dimerization constant of the mixed-valent state.[14] In the present system, these terms describe the thermodynamics of formation and stability of hydrogen-bonded species in the three possible redox states. Direct comparison of K_{MV} to K_D or K_{2-} allows determination of the relative degree of stability gained from charge transfer *across* a hydrogen bond.

Applying these ideas (see the Supporting Information for details),[14] we find that in DCM solutions, **1** is found to exist primarily as monomers, with a dimerization constant of K_D = 360 M^{-1} in the isovalent neutral state. The dimerization constant for the doubly reduced state (K_{2-}) is much more difficult to determine but can be estimated from the electrochemical experiments. The observation of a return oxidation in both CVs and DPVs near $E_{1/2}$ = −1.45 V vs $Fc^{+/0}$ corresponding to oxidation of singly reduced monomers, $(\mathbf{1})^-$, suggests that the doubly reduced state is weakly hydrogen-bonded and that a small amount dissociates into reduced monomers upon its formation. However, the fact that an appreciable amount of dimer is observed in the DPV trace upon the return oxidation (Figure S2) suggests that a majority of the complex is still dimerized. By comparison with the isonicotinic acid systems, where monomer reoxidation was not observed and K_{2-} was experimentally determined to be 2200 M^{-1}, we estimate that K_{2-} is on the order of 1000 M^{-1} for $(\mathbf{1}_2)^{2-}$.[14]

With the relevant formation constants known, K_{MV} is determined by the use of eq 2:[14]

$$K_{MV} = (K_D K_2 - K_C)^{1/2} \quad (2)$$

For complex **1**, K_{MV} is found to be 4 orders of magnitude larger than K_D and 3 orders of magnitude larger than K_{2-} with an approximate value of 5×10^6 M^{-1}. The relative stability of the mixed-valence state is revealed by inspection of the differences in the free energies corresponding to K_D, K_{2-}, and K_{MV} (Table 1). Here the mixed-valent state is estimated to be 5.7 kcal/mol (1980 cm^{-1}) and 5.1 kcal/mol (1784 cm^{-1}) more stable than the isovalent neutral and doubly reduced states, respectively (Figure 3). These results suggest a strongly delocalized electronic structure in the mixed-valent state that extends from the Ru_3O redox centers, through the π system of the pyrimidinone ligands, and across their hydrogen bonds.

Perhaps the most remarkable aspect of the mixed-valent pyrimidinone hydrogen-bonded complexes is that they exhibit significantly broadened, partially coalesced ν(CO) bands in their FTIR spectra (Figure 3). This behavior has not been previously observed in a mixed-valent hydrogen-bonded complex and allows estimation of the rate of ET by application of a Bloch equation line shape analysis, a well-documented procedure for the covalently bridged pyrazine clusters that have been extensively studied in our lab.[17−19] Simulation of the FTIR line shape proceeded through the use of the MATLAB program Zoerbex developed by the Harris lab.[20] The dynamic

DOI: 10.1021/jacs.8b09273
J. Am. Chem. Soc. 2018, 140, 12756−12759

Table 1. Equilibrium Dimerization Constants for 1 and the Analogous Isonicotinic Acid Cluster in DCM at 25°C

bridging ligand	K_D (M^{-1})	K_{2-} (10^3 M^{-1})	K_C (10^6)	K_{MV} (10^6)	$\Delta\Delta G_D^{\circ}$ [a] (kcal/mol)	$\Delta\Delta G_{2-}^{\circ}$ [b] (kcal/mol)
pyrimidinone	360	1	70	5	−5.7	−5.1
isonicotinc acid	75	2.2	3.2	0.7	−5.4	−3.2

[a] $\Delta\Delta G_D^{\circ} = \Delta G_{MV}^{\circ} - \Delta G_D^{\circ}$. [b] $\Delta\Delta G_{2-}^{\circ} = \Delta G_{MV}^{\circ} - \Delta G_{2-}^{\circ}$.

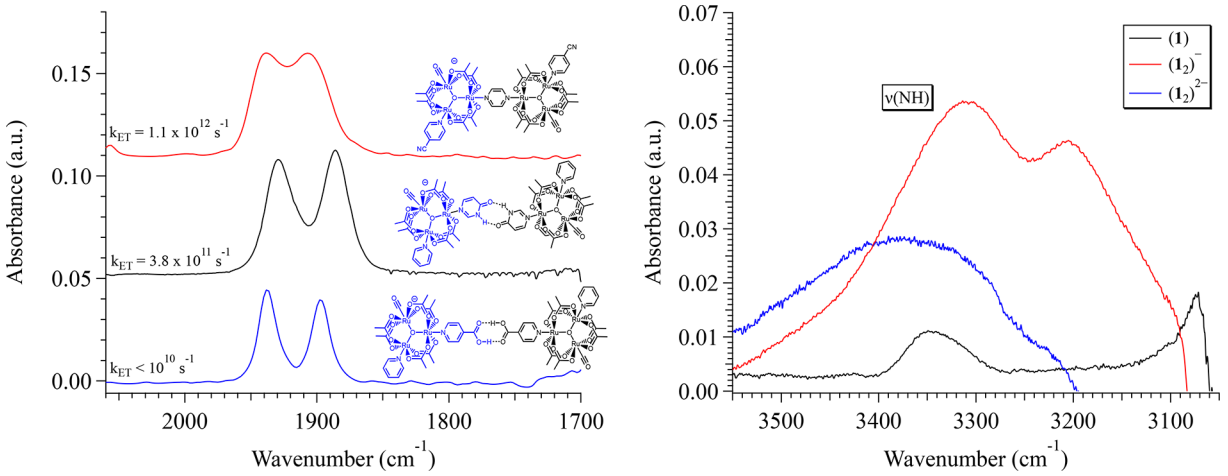

Figure 3. (left) Infrared spectroelectrochemical (IRSEC) spectrum of **1** (black, 4.85 mM) with the potential fixed at −1200 mV. Also shown for comparison are the IRSEC spectra of the corresponding isonicotinic acid-bridged clusters (blue) and the covalently linked pyrazine-bridged clusters (red). (right) IRSEC spectra of **1** (4.85 mM), highlighting the enormous intensity enhancement of the ν(NH) band in the mixed-valent hydrogen-bonded state (red) in comparison with the isovalent neutral (black) and doubly reduced (blue) states.

FTIR line shapes in the program are simulated using the optical Bloch formalism, where two species exchange 100% of their intensity at a rate k_{ex}. The program simulates vibrational spectra by Fourier transformation of the vibrational time correlation function into the frequency domain. Simulated FTIR spectra are represented as Voigt line shapes where the center peak frequencies, the Gaussian and Lorentzian fwhm values, the populations of the exchanging species, and their exchange time constant are taken as inputs.

To best determine the input parameters, the infrared spectroelectrochemical spectrum was fit to two well-resolved Voigt functions (Figure S9), whose parameters were then taken as the input for the Zoerbex program. The exchange time constant, τ, was manipulated until the simulated spectra were in good agreement with the experimental one (Figure S9). The best agreement between experiment and theory was found when the exchange time constant was set to 2.6 ps, giving rates of electron transfer near 3.8×10^{11} s^{-1}. These estimates are in excellent agreement with those of similar Ru_3O systems, where the predicted rate of ET in **1** falls between those for the more weakly coupled isonicotinic acid systems and the more highly coupled pyrazine-bridged systems (Figure 3). It is important to note that the application of such an analysis has been heavily debated in the literature,[21−24] as many processes in addition to chemical exchange, such as inhomogeneous broadening, solvent environment fluctuation and other dynamic processes, can contribute to the overall FTIR line shape. Until these systems can be the subjects of higher-order spectroscopic analysis, and in view of the well-documented nature of ultrafast ET in similar mixed-valent Ru_3O systems,[17−19] the methods here provide a reasonable first estimate of k_{ET}.

The nature of electron delocalization in these highly coupled mixed-valent hydrogen-bonded complexes is also partly revealed by the observation of an enormous intensity enhancement of the pyrimidinone amide ν(NH) band (3350 cm^{-1}) in the IR spectrum of the mixed-valent hydrogen-bonded state. The intensification of the ν(NH) band is absent in the neutral and doubly reduced states (Figure 3). On the basis of previous studies of the pyrazine (pz)-bridged dimers of trimers (Ru_3O−pz−Ru_3O),[19,25−27] this is a signature of strong vibronic coupling of the pyrimidinone amide ν(NH) mode with the Ru_3O electronic wave functions in the mixed-valent state. It may be an important promoter mode for ET.[28−30]

In conclusion, together these findings demonstrate the presence of strong donor−bridge−acceptor coupling across hydrogen bonds and that highly delocalized electronic structures can be attained in non-covalent assemblies that are often considered to be too weakly bound to support strong electronic communication. A forthcoming study will detail the nature of electronic and vibronic coupling in these systems through variation of the cluster electronics by ancillary ligand substitution and consideration of kinetic isotope effects.

■ ASSOCIATED CONTENT

Supporting Information

The Supporting Information is available free of charge on the ACS Publications website at DOI: 10.1021/jacs.8b09273.

Experimental details and additional electrochemical, infrared, and electronic spectra pertaining to the presented system (PDF)

■ AUTHOR INFORMATION

Corresponding Author

*ckubiak@ucsd.edu

ORCID

Tyler M. Porter: 0000-0002-2693-2653

Clifford P. Kubiak: 0000-0003-2186-488X

DOI: 10.1021/jacs.8b09273
J. Am. Chem. Soc. 2018, 140, 12756−12759

Author Contributions

[†]T.M.P. and G.P.H. contributed equally.

Notes

The authors declare no competing financial interest.

■ ACKNOWLEDGMENTS

We thank Dr. Anthony Mrse of the UCSD NMR facility for assistance and gratefully acknowledge support from NSF Grants CHE-1461632 and CHE-1759460.

■ REFERENCES

(1) Marcus, R. A.; Sutin, N. Electron transfers in chemistry and biology. *Biochim. Biophys. Acta, Rev. Bioenerg.* **1985**, *811* (3), 265−322.
(2) Ramirez, B. E.; Malmström, B. G.; Winkler, J. R.; Gray, H. B. The currents of life: the terminal electron-transfer complex of respiration. *Proc. Natl. Acad. Sci. U. S. A.* **1995**, *92* (26), 11949−11951.
(3) Gray, H. B.; Winkler, J. R. Electron flow through proteins. *Chem. Phys. Lett.* **2009**, *483* (1−3), 1−9.
(4) Beratan, D. N.; Onuchic, J. N.; Hopfield, J. J. Electron tunneling through covalent and noncovalent pathways in proteins. *J. Chem. Phys.* **1987**, *86* (8), 4488−4498.
(5) Onuchic, J. N.; Beratan, D. N. A predictive theoretical model for electron tunneling pathways in proteins. *J. Chem. Phys.* **1990**, *92* (1), 722−733.
(6) Beratan, D. N.; Betts, J. N.; Onuchic, J. N. Protein electron transfer rates set by the bridging secondary and tertiary structure. *Science* **1991**, *252* (5010), 1285−1288.
(7) Beratan, D. N.; Onuchic, J. N.; Winkler; Gray, H. B. Electron-tunneling pathways in proteins. *Science* **1992**, *258* (5089), 1740−1741.
(8) Hinchliffe, P.; Sazanov, L. A. Organization of Iron−Sulfur Clusters in Respiratory Complex I. *Science* **2005**, *309* (5735), 771−774.
(9) Shih, C.; Museth, A. K.; Abrahamsson, M.; Blanco-Rodriguez, A. M.; Di Bilio, A. J.; Sudhamsu, J.; Crane, B. R.; Ronayne, K. L.; Towrie, M.; Vlček, A.; Richards, J. H.; Winkler, J. R.; Gray, H. B. Tryptophan-Accelerated Electron Flow Through Proteins. *Science* **2008**, *320* (5884), 1760−1762.
(10) Sun, F.; Huo, X.; Zhai, Y.; Wang, A.; Xu, J.; Su, D.; Bartlam, M.; Rao, Z. Crystal Structure of Mitochondrial Respiratory Membrane Protein Complex II. *Cell* **2005**, *121* (7), 1043−1057.
(11) Winkler, J. R.; Gray, H. B. Electron Flow through Metalloproteins. *Chem. Rev.* **2014**, *114* (7), 3369−3380.
(12) Gray, H. B.; Winkler, J. R. Long-range electron transfer. *Proc. Natl. Acad. Sci. U. S. A.* **2005**, *102* (10), 3534−3539.
(13) de Rege, P. J.; Williams, S. A.; Therien, M. J. Direct evaluation of electronic coupling mediated by hydrogen bonds: implications for biological electron transfer. *Science* **1995**, *269* (5229), 1409−1413.
(14) Porter, T. M.; Heim, G. P.; Kubiak, C. P. Effects of electron transfer on the stability of hydrogen bonds. *Chem. Sci.* **2017**, *8* (11), 7324−7329.
(15) Canzi, G.; Goeltz, J. C.; Henderson, J. S.; Park, R. E.; Maruggi, C.; Kubiak, C. P. On the Observation of Intervalence Charge Transfer Bands in Hydrogen-Bonded Mixed-Valence Complexes. *J. Am. Chem. Soc.* **2014**, *136* (5), 1710−1713.
(16) Goeltz, J. C.; Kubiak, C. P. Mixed Valency across Hydrogen Bonds. *J. Am. Chem. Soc.* **2010**, *132* (49), 17390−17392.
(17) Ito, T.; Hamaguchi, T.; Nagino, H.; Yamaguchi, T.; Kido, H.; Zavarine, I. S.; Richmond, T.; Washington, J.; Kubiak, C. P. Electron Transfer on the Infrared Vibrational Time Scale in the Mixed Valence State of 1,4-Pyrazine- and 4,4′-Bipyridine-Bridged Ruthenium Cluster Complexes. *J. Am. Chem. Soc.* **1999**, *121* (19), 4625−4632.
(18) Londergan, C. H.; Kubiak, C. P. Electron transfer and dynamic infrared-band coalescence: It looks like dynamic NMR spectroscopy, but a billion times faster. *Chem. - Eur. J.* **2003**, *9* (24), 5962−5969.
(19) Kubiak, C. P. Inorganic Electron Transfer: Sharpening a Fuzzy Border in Mixed Valency and Extending Mixed Valency across Supramolecular Systems. *Inorg. Chem.* **2013**, *52* (10), 5663−5676.
(20) Zoerb, M. C.; Harris, C. B. A Simulation Program for Dynamic Infrared (IR) Spectra. *J. Chem. Educ.* **2013**, *90* (4), 506−507.
(21) Lu, R.; Gan, W.; Wu, B.-h.; Zhang, Z.; Guo, Y.; Wang, H.-f. C−H Stretching Vibrations of Methyl, Methylene and Methine Groups at the Vapor/Alcohol (n = 1−8) Interfaces. *J. Phys. Chem. B* **2005**, *109* (29), 14118−14129.
(22) MacPhail, R. A.; Strauss, H. L. Can the Bloch equations describe the vibrational spectra of a reacting molecule? *J. Chem. Phys.* **1985**, *82* (3), 1156−1166.
(23) Strauss, H. L. Changes of the carbonyl stretching spectra with temperature. *J. Am. Chem. Soc.* **1992**, *114* (3), 905−907.
(24) Wood, K. A.; Strauss, H. L. The integrated intensities of chemically-exchanging vibrational bands as given by the Bloch equations. *Ber. Bunsen-Ges. Phys. Chem.* **1989**, *93* (5), 615−616.
(25) Londergan, C. H.; Kubiak, C. P. Vibronic participation of the bridging ligand in electron transfer and delocalization: New application of a three-state model in pyrazine-bridged mixed-valence complexes of trinuclear ruthenium clusters. *J. Phys. Chem. A* **2003**, *107* (44), 9301−9311.
(26) Londergan, C. H.; Rocha, R. C.; Brown, M. G.; Shreve, A. P.; Kubiak, C. P. Intervalence involvement of bridging ligand vibrations in hexaruthenium mixed-valence clusters probed by resonance Raman spectroscopy. *J. Am. Chem. Soc.* **2003**, *125* (46), 13912−13913.
(27) Londergan, C. H.; Salsman, J. C.; Ronco, S.; Kubiak, C. P. Infrared Activity of Symmetric Bridging Ligand Modes in Pyrazine-Bridged Hexaruthenium Mixed-Valence Clusters. *Inorg. Chem.* **2003**, *42*, 926−928.
(28) Williams, R. D.; Petrov, V. I.; Lu, H. P.; Hupp, J. T. Intramolecular Electron Transfer in Biferrocene Monocation: Evaluation of Franck−Condon Effects via a Time-Dependent Analysis of Resonance Raman Scattering in the Extended Near-Infrared. *J. Phys. Chem. A* **1997**, *101* (43), 8070−8076.
(29) Marin, T. W.; Homoelle, B. J.; Spears, K. G.; Hupp, J. T.; Spreer, L. O. Vibrational Coherence Due to Promoting Mode Activity in the Relaxation Dynamics of the Class III Mixed-Valence Molecule $[Ru_2TIEDCl_4]^+$. *J. Phys. Chem. A* **2002**, *106* (7), 1131−1143.
(30) Spears, K. G. Models for Electron Transfer with Vibrational State Resolution. *J. Phys. Chem.* **1995**, *99* (9), 2469−2476.

DOI: 10.1021/jacs.8b09273
J. Am. Chem. Soc. 2018, 140, 12756−12759